

UDC 539.12.04: 621.793: 548.73

## STRUCTURAL ENGINEERING OF NbN/Cu MULTILAYER COATINGS BY CHANGING THE THICKNESS OF THE LAYERS AND THE MAGNITUDE OF THE BIAS POTENTIAL DURING DEPOSITION

*O.V. Sobol*<sup>1</sup>, *A.A. Andreev*<sup>2</sup>, *V.A. Stolbovoy*<sup>2</sup>, *D.A. Kolesnikov*<sup>3</sup>,  
*M.G. Kovaleva*<sup>3</sup>, *A.A. Meylekhov*<sup>1</sup>, *H.O. Postelnyk*<sup>1</sup>, *A.V. Dolomanov*<sup>2</sup>,  
*Yu.Ye. Sagaidashnikov*<sup>1</sup>, *Zh.V. Kraievska*<sup>1</sup>

<sup>1</sup>*National Technical University "Kharkiv Polytechnic Institute",  
Kharkiv, Ukraine*

*E-mail: sool@kpi.kharkov.ua;*

<sup>2</sup>*National Science Center "Kharkov Institute of Physics and Technology", Kharkiv, Ukraine*

*E-mail: aandreev@kipt.kharkov.ua;*

<sup>3</sup>*Belgorod State National Research University, Belgorod, Russian Federation*

To determine the patterns of structural engineering of vacuum-arc coatings based on niobium nitride in the NbN/Cu multilayer composition, the effect of layer thickness and bias potential on the structural-phase state and physico-mechanical characteristics of vacuum-arc coatings was studied. It was found that the metastable  $\delta$ -NbN phase (cubic crystal lattice, structural type NaCl) is formed in thin layers (about 8 nm thick) regardless of  $U_b$ . With a greater thickness of the layers of niobium nitride (in the multilayer NbN/Cu composition), the phase composition changes from metastable  $\delta$ -NbN to the equilibrium  $\epsilon$ -NbN phase with a hexagonal crystal lattice. An increase in the bias potential during deposition from -50 to -200 V mainly affects the change in the preferential orientation of crystallite growth. The highest hardness (28.2 GPa) and adhesive resistance is achieved in coatings obtained at  $U_b = -200$  V with the smallest layer thickness. The highest hardness corresponds to the structurally deformed state in which the crystallite texture is formed with the [100] axis perpendicular to the growth surface, as well as a large microstrain (1.5%) in crystallites.

PACS: 81.07.Bc, 61.05.cp, 68.55.jm, 61.82.Rx

### INTRODUCTION

Currently, structural engineering is the basic method of creating materials with high functional characteristics [1, 2]. The main directions of structural engineering are associated with surface modification [3, 4]. Modification of the surface layers makes it possible to most efficiently use the properties of base materials and modified layers, saving costly and rare metals and alloys. Surface engineering combines several methods. This is a directional change in the physico-chemical properties of the surface layers of materials by deforming [5], modifying [6], applying single-layer [7], multiperiod [8, 9], multi-element [10] coatings and protective layers. Also various combined methods are used [11].

The possibilities of structural surface engineering in recent years have been significantly expanded by using highly non-equilibrium processes in ion-plasma and vacuum-arc technologies [12, 13]. As a result, it was possible to create artificial composite materials with ultrahigh hardness and strength [14–16].

In the vacuum-arc method, nitrides are the most technologically advanced for producing highly hard coatings [17, 12].

Among nitrides, great attention is paid to niobium nitride. This is due to the fact that niobium nitride (NbN) has a high melting point (about 2700 K), which is determined by the high Nb–N bond energy (14.81 eV) [18]. NbN-based coatings exhibit many interesting properties, such as high hardness and electrical conductivity, heat resistance and chemical inertness [19]. However, the strength properties of materials based on NbN

are not yet high enough. This is largely determined by the fact that, with a decrease in crystallite size of less than 100 nm (and this is the basis for increasing functional characteristics), the strength of the boundaries becomes the determining factor. In this regard, high properties can be achieved by creating a multilayer coating (where a material with a low miscibility, such as copper, is used as the second layer). It should be noted that the achievement of the highest hardness with a layer thickness of about 10 nm is characteristic of multilayer systems based on nitrides [20]. However, for medical use, the thickness of the layers can be significantly greater (more than 100 nm). In such a large range of layer thicknesses (10...100 nm), significant changes in the structural state occur [21]. Such changes are the basis of structural engineering and allow determining the deposition regimes to achieve optimal structural states (textures, phase composition, micro- and macrostrains, etc.) [22].

Therefore, the purpose of this work was to determine the possibilities of structural engineering of NbN/Cu coatings with a layer thickness of 8...120 nm. In addition to the layer thickness, the bias potential applied to the substrate ( $U_b$ ) was used as a parameter to influence the structure and properties.

### SAMPLES AND RESEARCH METHODS

Multilayer coatings were obtained by the vacuum-arc method on the upgraded installation "Bulat-6". The pressure of the working (nitrogen) atmosphere during the deposition was  $P_N = 7 \cdot 10^{-4}$  Torr. The deposition was

carried out from two sources (Nb and Cu) on metal substrates in the modes of continuous and discrete rotation of the substrate holder with the substrates. With continuous rotation of samples fixed on the substrate at a speed of 8 rpm, the thickness of the layers was about 8 nm. In the discrete mode of layer deposition, the stopping time at the target corresponded to the specified thickness of the layers. The total coating deposition time was 1.5 h. The thickness of the coating was about 12  $\mu\text{m}$ . In the process of deposition, a constant negative bias potential ( $U_b$ ) of -50 and -200 V was applied to the substrates. The main modes of obtaining the coatings are given in Table 1.

Table 1

Cathode material and coating deposition parameters

Serial No.	Cathode Materials	$U_b$ , V	Layer deposition time, s
1	Cu/Nb	50	continuous
2	Cu/Nb	200	continuous
3	Cu/Nb	50	20
4	Cu/Nb	200	20
5	Cu/Nb	50	60
6	Cu/Nb	200	60
7	Cu/Nb	50	120
8	Cu/Nb	200	120

The phase-structural state was studied on a DRON-4 diffractometer in Cu- $K_\alpha$ -radiation. For monochromatization of the recorded radiation, a graphite monochromator was used, which was installed in the secondary beam (in front of the detector) [23]. The survey was carried out in the range of angles  $2\theta = 20 \dots 90^\circ$ . All diffraction peaks from the planes with the highest reticular density of atoms fall into this angular range. Scan step  $\theta = 0.02^\circ$ .

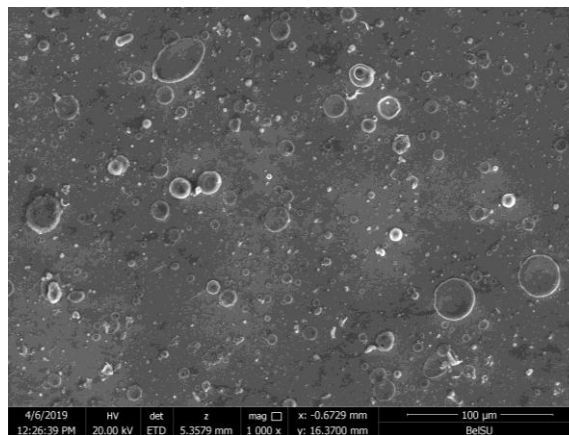
The study of the surface morphology of the obtained coatings was carried out using a scanning electron microscope FEI Nova NanoSEM 450. The elemental composition of the samples was studied by analyzing the spectra of the characteristic x-ray radiation generated by the electron beam in a scanning electron microscope. The spectra were taken with an PEGASUS energy dispersive X-ray spectrometer of EDAX company installed in a microscope.

The hardness was measured on a UHL VMHT microhardness meter with a load of 200 mN. The results were averaged over 12 measurements.

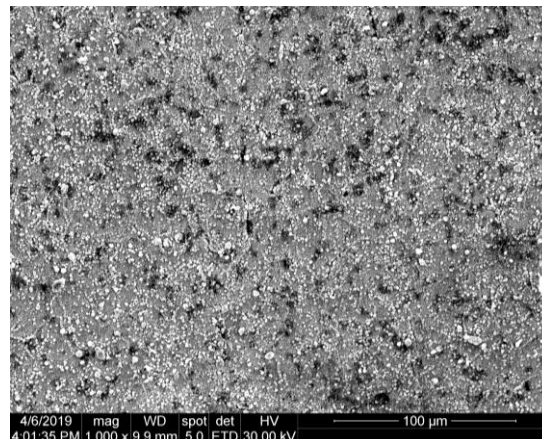
Determination of adhesive and cohesive strength, resistance to scratching and elucidation of the mechanism of destruction of coatings was carried out using a scratch tester Revetest (CSM Instruments).

## RESULTS AND DISCUSSION

The study of surface morphology showed that for coatings obtained at  $P_N = 7 \cdot 10^{-4}$  Torr, an increase in the bias potential from -50 V (Fig. 1,a) to -200 V (see Fig. 1,b) leads to a decrease in the size of surface inclusions (droplet phase). In this case, the magnitude of the largest inclusions of the droplet phase decreases from 15...20  $\mu\text{m}$  (see Fig. 1,a) to 5...7  $\mu\text{m}$  (see Fig. 1,b).



a



b

Fig. 1. The morphology of the coating surface which was deposited in a continuous mode at a bias potential of  $U_b = -50$  V (a) and -200 V (b)

Analysis of the lateral section of the coating obtained at the time of deposition of the layer is 60 s about 25 nm (Fig. 2). Thus, taking into account the secondary sputtering process, the growth rate of NbN layers is about 0.85 nm/s, and Cu layers about 0.45 nm/s.

The lateral section of the coating obtained at a lower bias potential of -50 V (series 5) is shown in Fig. 2,b. Taking into account the scale of the image, the thickness of the layers for NbN (light layers) is about 67 nm, and for Cu (dark layers) – 78 nm, respectively. Thus, at a low bias potential of -50 V, the deposition rate of NbN layers is about 1.1 nm/s, and for Cu it is about 1.3 nm/s.

The second important characteristic of coatings is their composition. Determination of the composition of the coatings was carried out by the method of energy dispersive analysis. The obtained data of elemental analysis (based on the energy dispersion spectra) are given in Table 2.

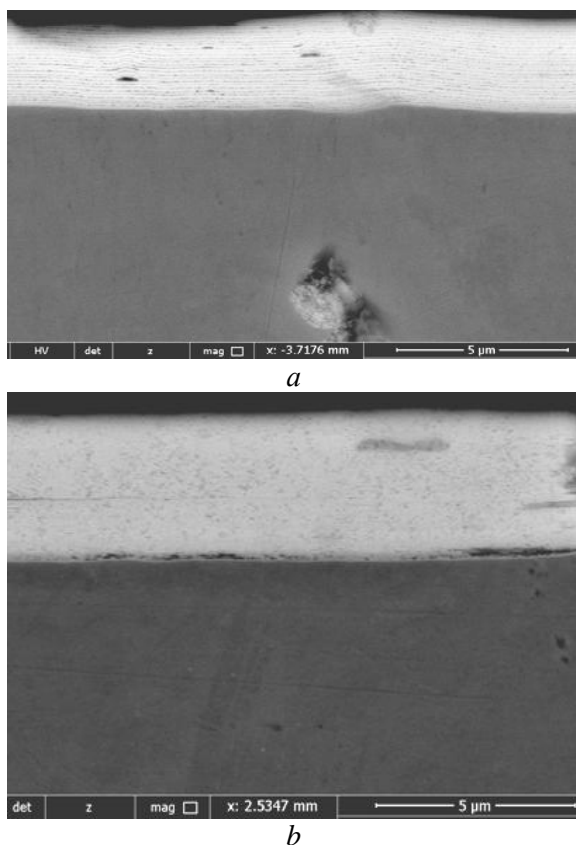


Fig. 2. SEM images of the lateral section of the coatings deposited at  $U_b = -200$  V (a) and  $-50$  V (b)

Table 2  
Elemental composition of multi-period NbN/Cu coatings

Series No.	The content of the element, at. %			N/Nb Ratio
	Nb	Cu	N	
1	31.5	46.4	22.1	0.70
2	46.5	11.2	42.3	0.91
3	34.6	40.8	24.6	0.71
4	45.5	20.8	33.7	0.74
5	31.5	44.8	23.7	0.75
6	44.1	24.4	31.3	0.71

As can be seen from the results in Table 2, with a relatively low negative bias potential of  $-50$  V (series 1, 3, and 5), a change in the deposition time has practically no effect on the ratio of elements. In significant measure, such a change is observed in the coatings that were deposited, with a higher bias potential of  $-200$  V. For a deposition time of 60 s (series 6), the ratio of Nb and Cu atoms is about 2. This agrees well with the results of determining the thickness of the layers by analyzing the SEM image of the side section (see Fig. 2). Even more as a result of sputtering, the relative content of heavier Nb atoms in the thinnest layers increases with continuous rotation (see Table 2).

The phase composition, structure and substructural characteristics were determined by the XRD method. Diffraction spectra of coatings deposited with continuous rotation of the substrate holder are shown in Fig. 3.

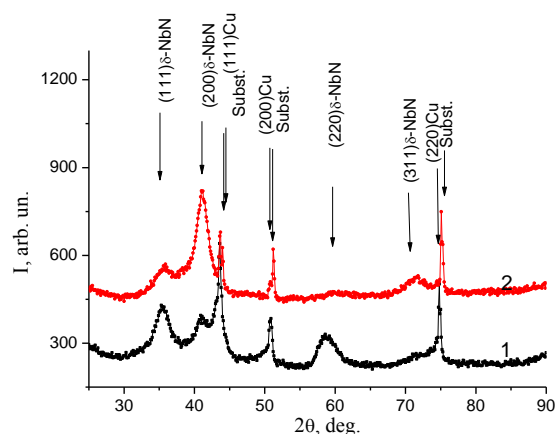


Fig. 3. X-ray diffraction spectra of NbN/Cu multilayer coatings obtained with  $U_b$ : 1 – 50 V; 2 – 200 V

With the smallest average layer thickness (about 8 nm, continuous rotation of the substrate holder), multiperiod coatings were obtained that may have superlattice properties (inheritance of the type and orientation of crystal lattices in adjacent layers). When this occurs, the formation of the metastable  $\delta$ -NbN phase with an fcc lattice (with a lattice of the same type as compared with the Cu layer). In this case, at a small value of  $U_b = -50$  V, all the diffraction peaks from the planes of the  $\delta$ -NbN phase lattice are reflected. The ratio of the peaks is close to the standard for the fcc lattice (structural type of NaCl). This indicates the absence of a pronounced texture. An increase in the bias potential of  $U_b$  to  $-200$  V leads to the appearance of an axis [100] with a preferential orientation of crystallite growth (see spectra 1 and 2 in Fig. 3).

Coatings with the greatest thickness of layers (series 7 and 8) have diffraction spectra presented in Fig. 4. As can be seen from the figure, an equilibrium  $\epsilon$ -NbN phase is formed in nitride layers. This condition is detected for various  $U_b$ . The only difference is in a different type of primary orientation of crystallites. In the case of low  $U_b = -50$  V, a pronounced texture axis is not detected. At that time, as with a large  $U_b = -200$  V, a texture appears with a (110) plane parallel to the growth surface (see Fig. 4, spectrum 2).

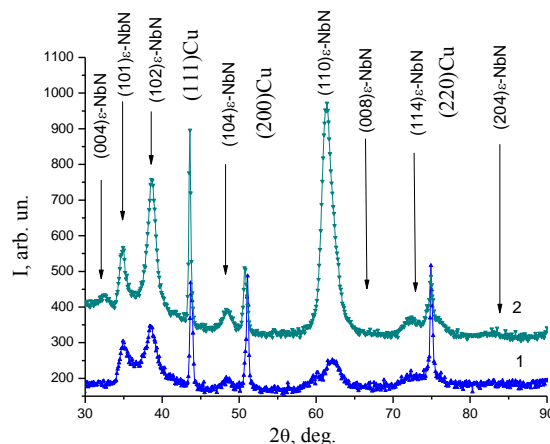


Fig. 4. X-ray diffraction spectra of NbN/Cu multilayer coatings with the highest layer thickness:

1 –  $U_b = -50$  V; 2 –  $U_b = -200$  V

The next stage of structural engineering is based on the possibilities of changing the structural state at different layer thicknesses. For these conditions, we consider the systematization by two main parameters:  $U_b$  and the layer thickness. The first series (at  $U_b = -50$  V) includes coatings with diffraction spectra 1, 3, and 5 in Fig. 5. The second series (at  $U_b = -200$  V) includes coatings with diffraction spectra of 2, 4, and 6 in Fig. 5. It can be seen that for a coating with thin layers (spectrum 1) a metastable  $\delta$ -NbN phase with a cubic lattice is formed. Increasing the layer thickness to 20 nm (spectrum 3) leads to the formation of only the equilibrium  $\varepsilon$ -NbN phase.

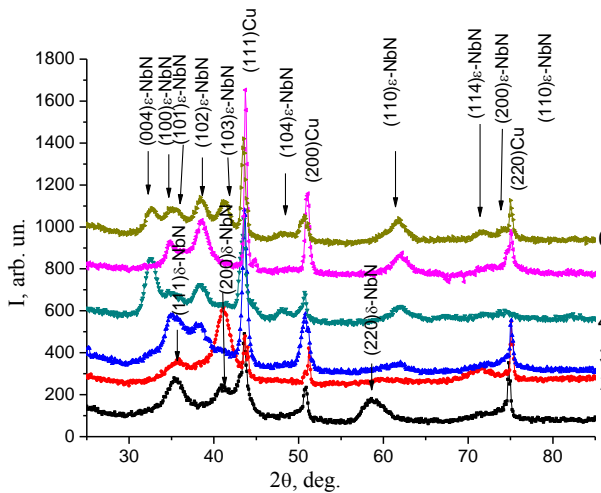


Fig. 5. X-ray diffraction spectra of NbN/Cu coatings: 1 –  $U_b = -50$  V (continuous rotation); 2 –  $U_b = -200$  V, continuous rotation; 3 –  $U_b = -50$  V, mode 20 s; 4 –  $U_b = -200$  V, mode 20 s; 5 –  $U_b = -50$  V, mode 60 s; 6 –  $U_b = -200$  V, mode 60 s

The appearance of the  $\varepsilon$ -NbN phase indicates that the deformation factor (associated with the growth in adjacent layers of structures with isotypic fcc lattices and coherent boundaries) exceeds the critical value. In this case, the striving of the system to a minimum of free energy stimulates the growth of the equilibrium  $\varepsilon$ -NbN phase. The formation of this phase is also characteristic of a large layer thickness (about 60 nm, spectrum 5).

For the second series (in coatings obtained at  $U_b = -200$  V), a similar change in the phase composition appears. The main difference of the coatings obtained at  $U_b = -200$  V is the formation of the preferential orientation of crystallite growth. At the smallest layer thickness (series 2), for the  $\delta$ -NbN phase, the crystallites are predominantly oriented with the [100] axis perpendicular to the growth plane. For thicker layers in which the  $\varepsilon$ -NbN phase is formed, one can distinguish a preferential orientation with a (004) plane parallel to the growth plane (at a layer thickness of about 20 nm) and a full spectrum of diffraction peaks without a noticeable preferential orientation – at a layer thickness close to 60 nm.

Substructural characteristics (crystallite size and microstrain) were analyzed depending on the layer thickness. It has been established that the general trend is an increase in the average crystallite size with an increase in the thickness of the layers. The dependence of the

microstrain on the thickness of the layers was revealed to be nonmonotonic.

Fig. 6 shows the results of determining the magnitude of microdeformation in the layers of niobium nitride.

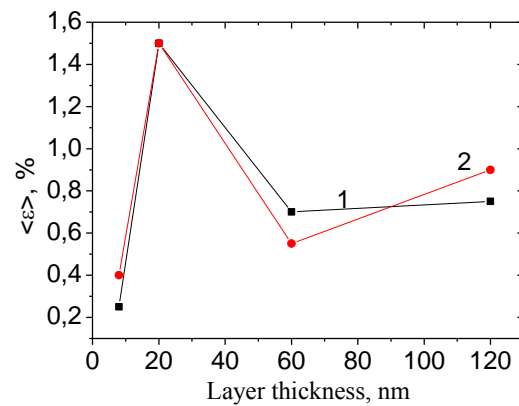


Fig. 6. Effect of layer thickness on the magnitude of microdeformation in the layers of niobium nitride: 1 – at  $U_b = -50$  V; 2 –  $U_b = -200$  V

As can be seen from Fig. 6, the crystal lattice is the most deformed in the layers, which are about 20 nm thick. This type of dependence can be explained by the fact that with the smallest layer thickness, the mixing of layers at the boundary is of great importance. This leads to a significant relaxation of the deformed state. In thick layers, considerable relaxation also occurs, but in this case its mechanism is different. It is determined by the appearance of dislocations and plastic strain relief. In layers with a thickness of about 20 nm, relaxation processes are difficult, since on the one hand the contribution of mixed boundary layers becomes insignificant, and on the other hand there is no possibility of relaxation by the dislocation mechanism (since the size of the layers is about 20 nm, which is smaller than the critical size for the source of dislocations Frank Reid). In this case, there is no possibility of the origin of dislocations.

The most universal characteristic of mechanical properties is hardness. The work was determined hardness for samples of various series. The results are shown in Fig. 7.

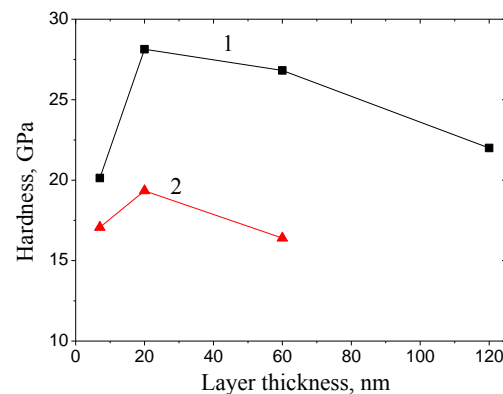


Fig. 7. Dependence of the hardness of coatings on the thickness of the layers: 1 –  $U_b = -200$  V; 2 –  $U_b = -50$  V

It is seen that the coatings obtained at a high bias potential of -200 V have a greater hardness than coatings



that were obtained with a lower bias potential of -50 V (see Fig. 7). It can also be seen that as the thickness of the layers increases to 20 nm, the hardness increases, and with a greater thickness, it decreases. If a comparison is made with the previously obtained data on the analysis of the phase composition and substructural characteristics, then it can be concluded that an increase in hardness is an increase in microstrain in layers with a thickness of about 20 nm (see Fig. 6).

The second important characteristic of mechanical properties of coatings is their adhesive strength. In work for its definition the method of scratch testing was used. Studies have shown that coatings with the lowest layer thickness (series 1 and 2) showed the highest adhesive strength.

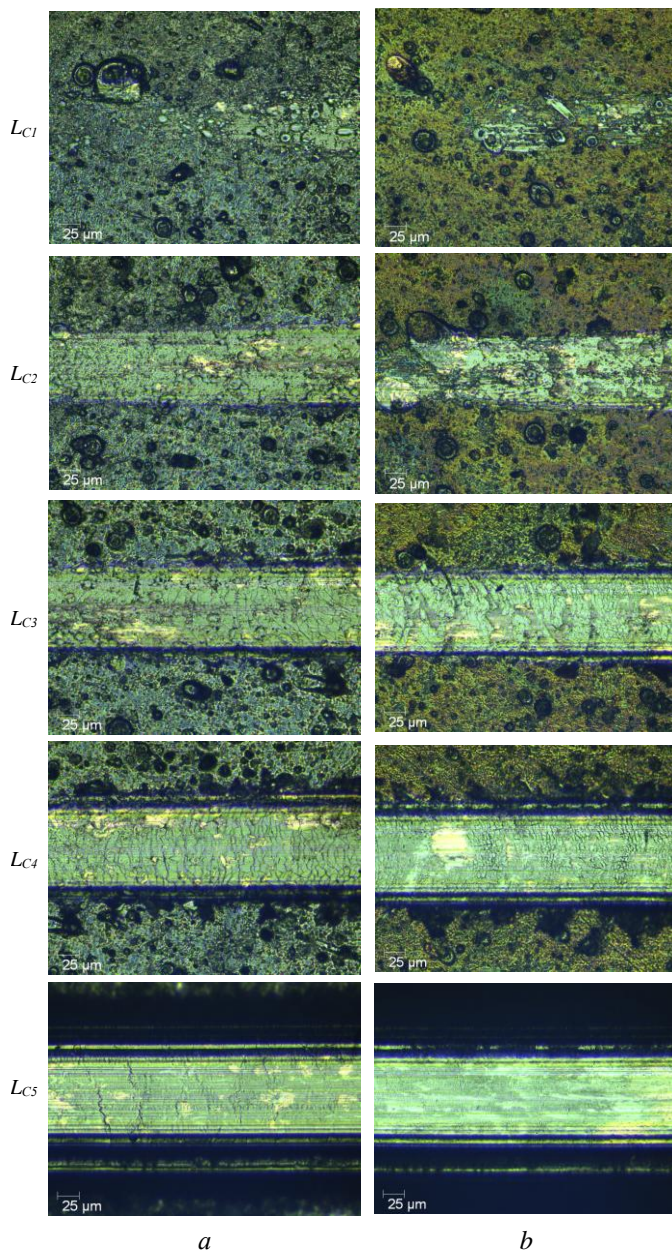


Fig. 8. Wear tracks in the areas of critical points under  $L_C$  loading for coatings obtained with: a –  $U_b = -50$  V (series 1); b –  $U_b = -200$  V (series 2)

Fig. 8 shows the wear tracks in the area of critical points  $L_C$  under loading (for series 1 and 2). The resulting data for the critical points for these areas are shown in Table 3. The contact load was 0.9 N, and the loading rate was 5 N/s.

Table 3

The magnitude of the load in the area of critical points  $L_C$

Series No	$L_C, H$				
	1	2	3	4	5
1	23.85	30.31	35.33	40.12	96.52
2	20.97	26.60	31.98	37.12	121.03

It can be seen that in the field of the formation of primary cracks (the critical point  $L_{C1}$ ), the coatings obtained at  $U_b = -50$  V have greater strength. This tendency persists for the critical points  $L_{C2}$ ,  $L_{C3}$ , and  $L_{C4}$ , when complexes of cracks and the initial separation of the coating parts are formed. However, the critical point  $L_{C5}$  (the load at which complete abrasion of the coating occurs) is higher for series 2 (obtained at  $U_b = -200$  V). This can be associated with a higher hardness characteristic of such coatings.

## CONCLUSIONS

1. It has been established that an increase in the bias potential from -50 to -200 V leads to an increase in the homogeneity of the surface growth morphology of the coating and a decrease in the size of droplet inclusions.

2. At a low bias potential,  $U_b = -50$  V for all layer thicknesses, the ratio of the elements does not undergo significant changes. The deposition rate is about 1.1 nm/s for NbN and 1.3 nm/s for Cu. In coatings obtained with a higher bias potential of -200 V, the relative content of Nb atoms (as compared to Cu) increases. The reason for this is the selective sputtering of lighter Cu atoms from the surface during the formation of the coating. As a result, the effective deposition rate is 0.85 nm/s for NbN layers, and 0.45 nm/s for Cu layers.

3. The critical layer thickness ( $\leq 20$  nm) was established at which the metastable  $\delta$ -NbN phase is formed (cubic crystal lattice, structural type NaCl). With a greater thickness of the layers of niobium nitride (in the multilayer NbN/Cu composition), the phase composition changes from the metastable  $\delta$ -NbN phase to the equilibrium  $\epsilon$ -NbN phase with a hexagonal crystal lattice.

4. An increase in the bias potential during deposition from -50 to -200 V mainly affects the change in the preferential orientation of crystallite growth. In thin layers of the  $\delta$ -NbN phase, a crystallite texture with the [100] axis is formed. In layers with a thickness of 40...60 nm, crystallites of the  $\epsilon$ -NbN phase with the plane of the (004) hexagonal lattice parallel to the growth plane are predominantly formed. At the maximum layer thickness (about 120 nm), the predominant formation of crystallites of the  $\epsilon$ -NbN phase occurs with the (110) plane of the hexagonal lattice parallel to the growth plane.

5. At the substructural level, as the thickness of the layers increases, the crystallite size increases. The dependences of the microstrain on the thickness of the layers have a non-monotonic appearance with a maximum (about 1.5%) at a layer thickness of 20 nm.

6. The hardness of coatings obtained at a bias potential of -200 V is higher than that obtained with a potentiation bias of -50 V. The reason for this may be an increase in the specific content of NbN in coatings obtained at a bias potential of -200 V.

7. The highest hardness of 28.2 GPa is achieved in coatings obtained at a bias potential of -200 V, and at a layer thickness of about 20 nm. The structure-deformed state, which corresponds to the highest hardness, is the texture of crystallites with the axis [100] perpendicular to the growth surface, as well as a large microstrain (1.5%) in crystallites.

8. The critical value of the load at failure has the highest value 121.03 N in the coatings with the highest hardness, obtained at  $U_b = -200$  V.

## REFERENCES

1. P.H. Mayrhofer, C. Mitterer, L. Hultman, H. Clemens. Microstructural design of hard coatings // *Progress in Materials Science*. 2006, v. 51, p. 1032-1114.
2. O.V. Sobol', A.A. Andreev, V.F. Gorban. Structural engineering of vacuum-arc multiperiod coatings // *Metal Science and Heat Treatment*. 2016, v. 58(1), p. 40-42.
3. M. Bourebia, L. Laouar, H. Hamadache & S. Dominiakn. Improvement of surface finish by ball burnishing: approach by fractal dimension // *Surface engineering*. 2017, v. 33(4), p. 255-262.
4. M. Bartosik, C. Rumeau, R. Hahn, Z.L. Zhang, P.H. Mayrhofer. Fracture toughness and structural evolution in the TiAlN system upon annealing // *Scientific Reports*. 2017, v. 7, p. 16476.
5. B.D. Morton, H. Wang, R.A. Fleming, M. Zou. Nanoscale surface engineering with deformation-resistant core-shell nanostructures // *Tribology letters*. 2011, v. 42(1), p. 51-58.
6. G. Maistro, S.A. Pérez-García, M. Norell, L. Nyborg, Y. Cao. Thermal decomposition of N-expanded austenite in 304L and 904L steels // *Surface engineering*. 2017, v. 33(4), p. 319-326.
7. L.R. Sheppard, H. Zhang, R. Liu, S. Macartney, T. Murphy, R. Wuhler. Reactive sputtered  $Ti_xNb_yN_z$  thin films. I. Basic processing relationships // *Materials Chemistry and Physics*. 2019, v. 224, p. 308-313
8. O.V. Sobol, A.A. Andreev, V.F. Gorban, A.A. Meylekhov, H.O. Postelnyk, V.A. Stolbovoy. Structural engineering of the vacuum-arc ZrN/CrN multilayer coatings // *Journal of Nano- and Electronic Physics*. 2016, v. 8(1), p. 01042.
9. O.V. Sobol', A.A. Andreev, V.F. Gorban', V.A. Stolbovoy, A.A. Meylekhov, A.A. Postelnyk, A.V. Dolomanov. Influence of pressure of working atmosphere on the formation of phase-structural state and physical and mechanical properties of vacuum-arc multilayer coatings ZrN/CrN // *Problems of Atomic Science and Technology*. 2016, v. 101(1), p. 134-139.
10. O.V. Sobol'. Nanostructural ordering in W-Ti-B condensates // *Physics of the Solid State*. 2007, v. 49(6), p. 1161-1167.
11. C. Czosnek, M.M. Bućko, J.F. Janik, Z. Olejniczak, M. Bystrzejewski, O. Łabędź, A. Huczko. Preparation of silicon carbide SiC-based nanopowders by the aerosol-assisted synthesis and the DC thermal plasma synthesis methods // *Mater. Res. Bull.* 2015, v. 63, p. 164-172.
12. *Nanostructured coatings* / Edited by: Cavaleiro, Albano; De Hosson, Jeff Th. M. Springer – Verlag, 2006, 648 p.
13. J. Xu, M. Kamiko, Y. Zhou, R. Yamoto, G. Li, and M. Gu. Superhardness effects of heterostructure NbN/TaN nanostructured multilayers // *Journal of Applied Physics*. 2001, v. 89, p. 3674-3678.
14. S. Veprek, S. Mukharjee, P. Karvankova, H.D. Maning, J.L. He, K. Moto, J. Prohazka, A.S. Argon. Limits to the strength of super- and ultra-hard nanocomposite coatings // *J. Vac. Sci. Technol.* 2003, v. A 21(3), p. 532-544.
15. J. Musil. Hard and superhard nanocomposite coatings // *Surface & Coatings Technology*. 2000, v. 125(1-3), p. 322-330.
16. S. Zhang, D. Sun, Y. Fu, H. Du. Toughness measurement of thin films: a critical review // *Surf. Coat. Tech.* 2005, v. 198, p. 2-8.
17. O.V. Sobol', A.A. Postelnyk, A.A. Meylekhov, A.A. Andreev, V.A. Stolbovoy, V.F. Gorban'. Structural engineering of the multilayer vacuum Arc nitride coatings based on Ti, Cr, Mo, and Zr // *Journal of Nano- and Electronic Physics*. 2017, v. 9(3), p. 03003.
18. А.И. Волков, И.М. Жарский. *Большой химический справочник*. Минск: «Современная школа», 2005, 608 с.
19. S.A. Barnett, A. Madan, I. Kom, K. Martin. Stability of nanometer-thick layers in hard coatings // *MRS Bull.* 2003, v. 28, p. 169-172.
20. O.V. Sobol', A.A. Meylekhov. Conditions of Attaining a Superhard State at a Critical Thickness of Nanolayers in Multiperiodic Vacuum-Arc Plasma Deposited Nitride Coatings // *Technical Physics Letters*. 2018, v. 44(1), p. 63-66.
21. R.A. Koshy, M.E. Graham, L.D. Marks. Synthesis and characterization of CrN/Mo<sub>2</sub>N multilayers and phases of Molybdenum nitride // *Surface & Coatings Technology*. 2007, v. 202, p. 1123-1128.
22. O.V. Sobol', A.A. Meylekhov, V.A. Stolbovoy, A.A. Postelnyk. Structural engineering multiperiod coating ZrN/MoN // *Journal of Nano- and Electronic Physics*. 2016, v. 8(3), p. 03039.
23. O.V. Sobol', O.A. Shovkoplyas. On advantages of X-ray schemes with orthogonal diffraction vectors for studying the structural state of ion-plasma coatings // *Technical Physics Letters*. 2013, v. 39(6), p. 536-539.

## **СТРУКТУРНАЯ ИНЖЕНЕРИЯ NbN/Cu МНОГОСЛОЙНЫХ ПОКРЫТИЙ ПУТЕМ ИЗМЕНЕНИЯ ТОЛЩИНЫ СЛОЕВ И ВЕЛИЧИНЫ ПОТЕНЦИАЛА СМЕЩЕНИЯ ПРИ ОСАЖДЕНИИ**

*О.В. Соболев, А.А. Андреев, В.А. Столбовой, Д.А. Колесников, М.Г. Ковалева, А.А. Мейлехов, А.А. Постельник, А.В. Долманов, Ю.Е. Сагайдашников, Ж.В. Краевская*

Для определения закономерностей структурной инженерии вакуумно-дуговых покрытий на основе нитрида ниобия в многослойной композиции NbN/Cu изучены влияния толщины слоев и потенциала смещения на структурно-фазовое состояние и физико-механические характеристики вакуумно-дуговых покрытий. Установлено, что в тонких слоях (толщиной около 8 нм) вне зависимости от  $U_b$  происходит формирование метастабильной  $\delta$ -NbN-фазы (кубическая кристаллическая решетка, структурный тип NaCl). При большей толщине слоев нитрида ниобия (в многослойной композиции NbN/Cu) происходит изменение фазового состава от метастабильной  $\delta$ -NbN-фазы до равновесной  $\epsilon$ -NbN-фазы с гексагональной кристаллической решеткой. Увеличение потенциала смещения при осаждении от -50 до -200 В в основном влияет на изменение преимущественной ориентации роста кристаллитов. Наибольшая твердость (28,2 ГПа) и адгезионная стойкость достигаются в покрытиях, полученных при  $U_b = -200$  В и наименьшей толщине слоев. Наибольшей твердости соответствует структурно-деформированное состояние, при котором формируется текстура кристаллитов с осью [100], перпендикулярной поверхности роста, а также большая микродеформация (1,5%) в кристаллитах.

## **СТРУКТУРНА ІНЖЕНЕРІЯ NbN/Cu БАГАТОШАРОВИХ ПОКРИТТІВ ШЛЯХОМ ЗМІНИ ТОВЩИНИ ШАРІВ І ВЕЛИЧИНИ ПОТЕНЦІАЛУ ЗСУВУ ПРИ ОСАДЖЕННІ**

*О.В. Соболев, А.О. Андреев, В.О. Столбовой, Д.А. Колесников, М.Г. Ковальова, А.О. Мейлехов, Г.О. Постельник, А.В. Долманов, Ю.Е. Сагайдашников, Ж.В. Краевська*

Для визначення закономірностей структурної інженерії вакуумно-дугових покриттів на основі нітриду ніобію в багатошаровій композиції NbN/Cu досліджено впливи товщини шарів і потенціалу зсуву на структурно-фазовий стан і фізико-механічні характеристики вакуумно-дугових покриттів. Встановлено, що в тонких шарах (товщиною близько 8 нм) незалежно від  $U_b$  відбувається формування метастабільної  $\delta$ -NbN-фазы (кубична кристалічна решітка, структурний тип NaCl). При більшій товщині шарів нітриду ніобію (у багатошаровій композиції NbN/Cu) відбувається зміна фазового складу від метастабільної  $\delta$ -NbN-фазы до рівноважної  $\epsilon$ -NbN-фазы з гексагональною кристалічною решіткою. Збільшення потенціалу зсуву при осадженні від -50 до -200 В в основному впливає на зміну переважної орієнтації зростання кристалітів. Найбільша твердість (28,2 ГПа) і адгезійна стійкість досягаються в покриттях, отриманих при  $U_b = -200$  В і найменшій товщині шарів. Найбільшій твердості відповідає структурно-деформований стан, при якому формується текстура кристалітів з віссю [100], перпендикулярною поверхні зростання, а також велика мікродеформація (1,5%) у кристалітах.